Axial shift mapping metrology for X-ray telescope mirrors

Hayden J. Wisniewski[a], Ian J. Arnold[a], Ralf K. Heilmann[b], Mark L. Schattenburg[b],

Brandon D. Chalifoux*[a]

[a]James C. Wyant College of Optical Sciences, The University of Arizona, 1630 E University Blvd. Tucson, Az USA 85721;

[b]Space Nanotechnology Laboratory, MIT Kavli Institute for Astrophysics and Space Research, Massachusetts Institute of Technology, 77 Massachusetts Avenue, Cambridge, MA USA 02139

ABSTRACT

The next generation of high-resolution X-ray telescopes will require mirror segments characterized to 5 nm uncertainty or better. This is difficult to achieve due to the mirror segment's off-axis hyperbolic and parabolic shape and the challenge of manufacturing and testing a cylindrical null lens. In a typical Fizeau interferometer setup, errors in the assumed perfect null lens will be coupled into the final surface figure, increasing uncertainty. To combat the higher uncertainty of the cylindrical null corrector, we have been developing lateral shift mapping, an absolute metrology technique using a Fizeau interferometer. In this technique, the surface under test is laterally shifted between measurements while the reference surface does not move. Contributions to the interferogram due to the surface under test will move, while contributions due to the reference will stay static. Using this information, we can extract the true surface under test with low uncertainty. There is a quadratic ambiguity that arises due to the extraction method being akin to an integration. We have shown in the past our ability to utilize lateral shift mapping to extract flat surfaces to sub-nanometer uncertainties by comparing our results to a three-flat test. We also demonstrated that we can eliminate the quadratic ambiguity in flats using an external measurement with an autocollimator. We are expanding this method from optical flats to cylindrical surfaces, creating axial shift mapping. We will report on progress toward sub-nanometer measurements of cylindrical mirrors using axial shift mapping.

Keywords: X-ray telescope, X-ray mirrors, X-ray mirror metrology, absolute metrology, surface metrology, optical metrology.

*bchal@arizona.edu

1. INTRODUCTION

There are many ways to characterize the low-spatial frequency figure error of X-ray mirrors: X-ray pencil beam[1] or Hartmann[2] metrology, Fizeau interferometry with a refractive or diffractive cylindrical null[3,4,5], long trace profilometry[6,7], Shack-Hartmann wavefront sensing[8,9], and deflectometry[10]. Each method has its own set of advantages and disadvantages. For example, Fizeau interferometry is able to characterize the full surface in one measurement, easy to set up, and can be done at atmospheric pressures, but it is held back by the fact that you can only know the surface as well as you know the reference. The next generation of X-ray telescopes will have a performance goal of 0.5 arcsec half-power diameter on axis[11], which equates to a surface figure error better than 5 nm rms[12]. To achieve this with Fizeau interferometry, we will have to characterize the reference surface to much lower than 5 nm rms if we want the surface under test (SUT) to meet the performance requirement. Another option is to implement a method that removes the effect of the reference surface on the measurement of the SUT.

X-ray mirrors are difficult to characterize due to their off-axis parabolic and hyperbolic figures[13]. Absolute metrology methods are well known for optical spheres and flats[14,15], but these methods rely on point symmetry, which the acylindrical shapes of X-ray mirrors do not have. Along with only line symmetry, the axial figure of the mirror is the most important dimension for system performance. The axial figure and some common figure errors along that dimension can be seen in Figure 1. It is imperative that any method we develop can accurately measure the axial figure of the mirrors.

Here we present axial shift mapping (ASM), an absolute metrology technique aimed at extracting the SUT from a set of Fizeau measurements without the effects of the reference surface. As far as we are aware, this method was first described in 2010 for measurements of optical flats with a Fizeau interferometer[16,17], and we have confirmed our ability to recreate this method for flats down to sub-nanometer error with the quadratic term removed[18]. This paper focuses on the developments over the last year including a new way to reliably extract the quadratic term along the axial figure, and how we plan to expand this method to cylindrical surfaces.

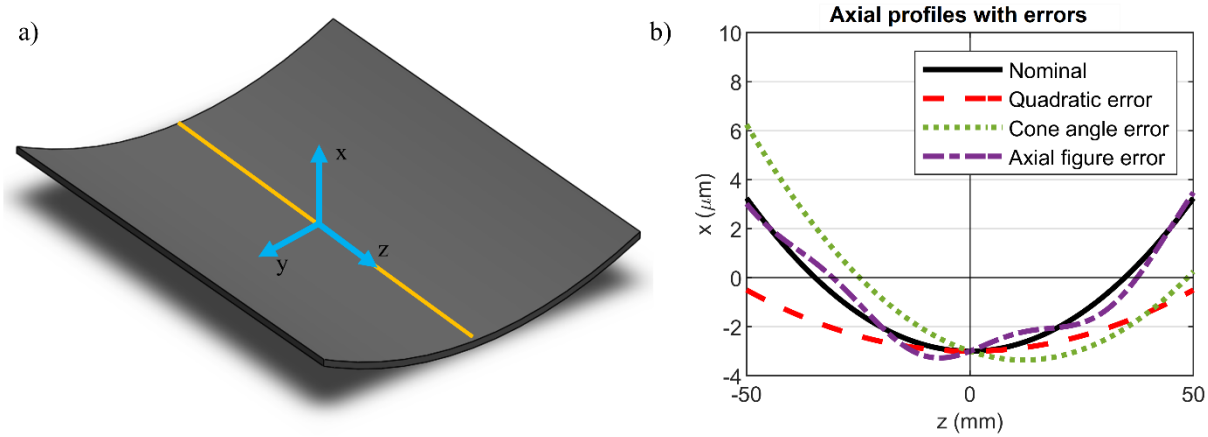

Figure 1. a) Rendering of an X-ray telescope mirror segment with a local coordinate frame. The axial figure is highlighted with an orange line. This dimension is critical for system performance, and it is imperative that we can accurately measure the quadratic term along this line. b) A visualization of the nominal axial figure and typical errors that can be seen in the axial figure.

2. METHOD

Axial shift mapping is a slope-based surface extraction technique with which we can separate out the reference surface from the surface under test by integrating from slope space. To obtain the slopes, the surface under test is shifted by the size of an interferometer CCD pixel when projected into object space. We use an Äpre instruments S100 Fizeau interferometer which has a projected pixel size of 50 μm, therefore our minimum step size is 50 μm. The full surface extraction relies on a minimum of three Fizeau measurements, two of which are shifted in orthogonal directions with respect to the nominal position. In this paper we present only one-dimensional extractions, meaning that only a shift in the direction of the extraction is required.

2.1 Extraction method

The description of the method has been presented before[18], and is repeated here as a review. In one dimension, we assume that the Fizeau measurement is the subtraction of the SUT and reference surface at each point (Figure 2). This is described as

$$m_{i,1} = S_i - R_i \tag{1}$$

where i is the pixel index, S is the contribution due to the surface, R is the contribution due to the reference, and m is the measurement at that index. The subscript 1 refers to this measurement being at the nominal position. When we shift the SUT by one pixel, we now obtain

$$m_{i,2} = S_{i+1} - R_i \tag{2}$$

where the shift is reflected in the subscript 2 on the measurement and the movement of what part of the SUT contributes to the measurement. During both Fizeau measurements, we will obtain data at each pixel. If we put all the measurements into a vector, where measurement 2 is appended to the end of measurement 1, we get

$$\vec{m} = [m_{1,1} \quad m_{2,1} \quad \cdots \quad m_{N,1} \quad m_{1,2} \quad m_{2,2} \quad \cdots \quad m_{N,2}]^{\mathrm{T}} \tag{3}$$

where N is the number of pixels. If we do a similar arrangement with the true surfaces that we are trying to solve for, we generate

$$\vec{z} = [R_1 \quad R_2 \quad \cdots \quad R_N \quad S_1 \quad S_2 \quad \cdots \quad S_N]^{\mathrm{T}} \tag{4}$$

and equation (3) and (4) can be related by a sparse matrix of **K** that represents equations (1) and (2). This can be written as

$$\mathbf{K} \cdot \vec{z} = \vec{m} \tag{5}$$

A single measurement informing our extraction is prone to errors, so to solve equation (5) we take more measurements, each shifted by one pixel in the measurement direction. These extra measurements are appended to the end of the *m* vector. We then use a Moore-Penrose inverse, a well-known least mean square method, on equation (5) to give

$$\vec{z} = (\mathbf{K}^{\mathrm{T}}\mathbf{K})^{-1}\mathbf{K}^{\mathrm{T}} \cdot \vec{m} \tag{6}$$

from which we can extract the true surfaces. We can shift more than one pixel at a time, it just requires the **K** matrix to be altered to reflect this variation to equation (2).

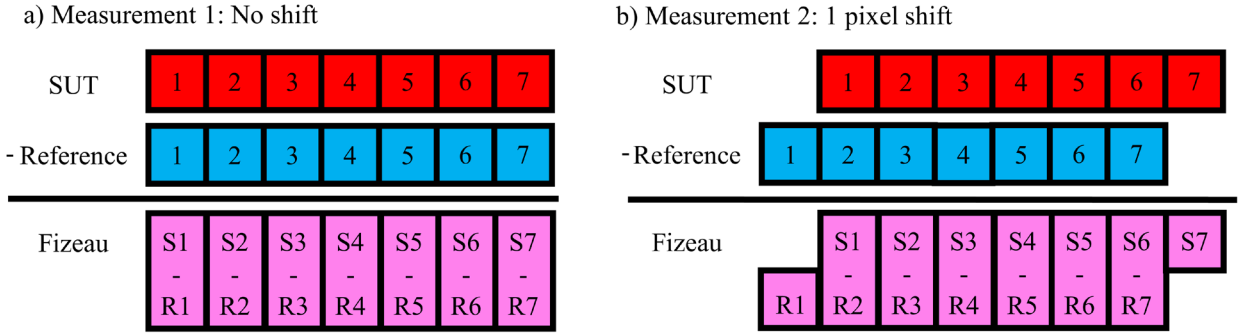

Figure 2. Diagram how we can use a one-pixel shift to remove contributions due to the reference surface. By taking a difference between the two Fizeau results, we eliminate the reference surface from the measurements as it remains stationary. We are left with a slope between pixel 1 and 2, both informed by the SUT. In practice we do these many times and use the least mean square method of a pseudoinverse matrix to mitigate errors.

2.2 Quadratic ambiguity

An issue that arises with slope space measurements is a loss of information due to a lack of uniqueness in slope space. This non-uniqueness comes from two or more different effects generating the same result when integrated. In axial shift mapping, a tilt of the surface during shifting will produce the same slope space difference as a quadratic surface when shifted, after the difference is taken according to equations. A diagram of this can be seen in Figure 3. This is of particular interest to the application of X-ray telescope mirrors, because along the line of extraction is the axial figure, which is crucial to system performance. Unlike mirrors that reflect light near normal-incidence, grazing-incidence mirrors cannot compensate for axial radius of curvature uncertainty using rigid body motions. Other methods of X-ray mirror metrology, like long-trace profilometry, are not blind to this term like axial shift mapping[7]. Standard Fizeau interferometry with an uncharacterized reference is blind to this quadratic term as well as higher order terms.

This requirement, along with the non-uniqueness, leads to the conclusion that an external measurement of some kind is required to accurately extract the surface. One method uses an autocollimator looking at a mirror that is rigidly attached to the side of SUT. This will measure tilts of the surface as it is translated. These tilts can then be removed before the surfaces are extracted, meaning that any quadratic we see in the surface is due to a real quadratic surface profile. The autocollimator has drawbacks in that it adds sources of errors such as autocollimator noise, alignment drift of the mirror it is looking at, and alignment drift of the interferometer reference flat. We have shown results using this method in the past, and will be comparing them to the second method. The method that we are showing here involves a second flat mirror in the field of view of the interferometer. This second mirror, which we are calling the reference mirror, is measured absolutely using a three-flat test before axial shift mapping measurements are made. Any tilts of the SUT during shifting can be extracted from what tilts we see in the profile of the premeasured reference mirror. This eliminates the noise of a second instrument looking at the surface, and any drift in the interferometer reference flat alignment affects both the SUT and reference mirror measurement, and therefore does not affect the extracted surface. This method also allows a smaller path between SUT and external reference mirror, mitigating some possible sources of errors from index of refraction

variations in air. This method has many potential benefits that may lead to a lower noise floor for axial shift mapping as a metrology method.

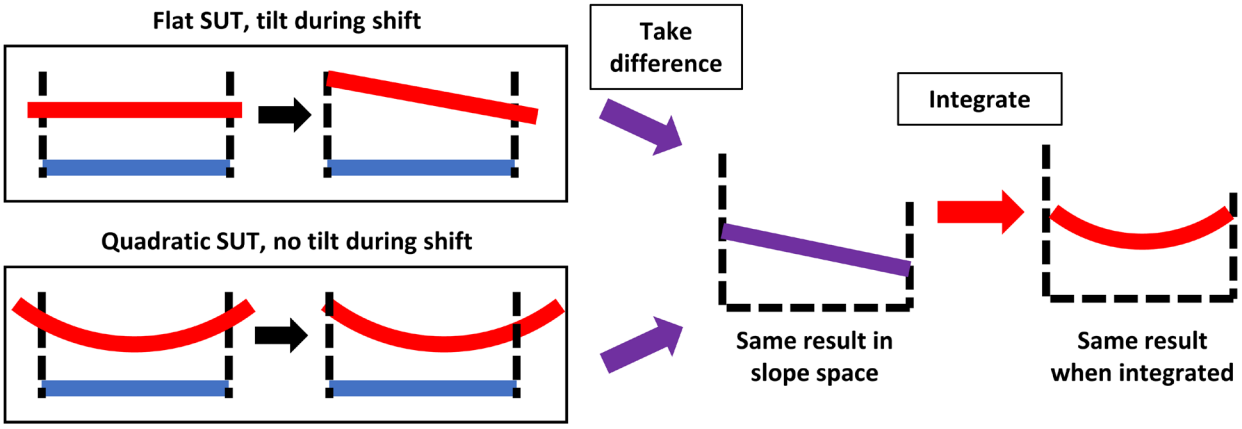

Figure 3. Example of how a tilt during shifting can give the same result as a quadratic that is not tilted. When taking a difference between measurements for both cases, they give the same result in slope space. This method is akin to an integration, and both examples give a quadratic when integrated. This results in an ambiguity as to whether the quadratic in the extracted surface is due to an actual quadratic term in the surface or a tilt during shifting.

3. EXPERIMENTAL SETUP

Ultra-low expansion (ULE) glass mirrors were used as our surface under test and our reference mirror. These mirrors were put into an aluminum mount which was then inserted into a precision tip/tilt mount on a 2-axis Aerotech stage. The mount included features to act as a fiducial to the centerline of the mirror. This aided in ensuring we were measuring the correct line during ASM measurements and three-flat test measurements. All measurements were taking using an Äpre Instruments S100 Fizeau interferometer. This portion of the system can be seen in Figure 4. Not pictured is the autocollimator we used to make tilt measurements. Despite having the reference mirror, we included the autocollimator because we wanted to compare our reference mirror method of quadratic extraction to our previous method of using an autocollimator. The autocollimator was rigidly attached to the optical table on a granite slab. The autocollimator mirror was mounted in a low-drift mirror mount and attached to the tip/tilt stage facing along the direction of shifting.

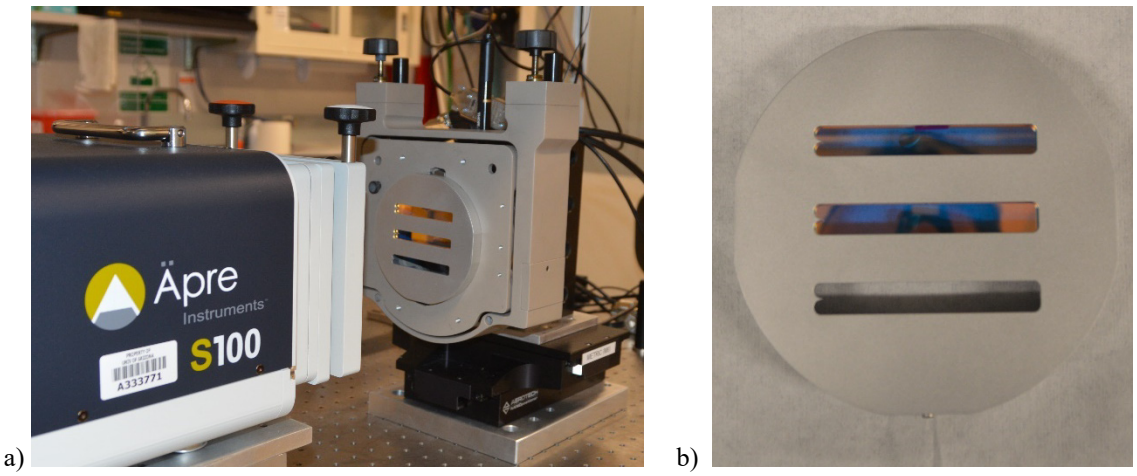

Figure 4. Experimental set up with Äpre S100 Fizeau interferometer (*a*) looking at the mirror mount (*b*) which holds the surface under test (*center of mount*) and the known reference mirror (*top of mount*). This mount is in a precision tip-tilt stage attached to an Aerotech X-Y stage. The reference mirror is measured beforehand using a basic three flat test.

4. RESULTS

Extracted surfaces and their errors are shown below. All three different results are from the same set of raw data. What sets them apart is the method used to determine the quadratic term of the SUT. The first extraction shown (Figure 5) is using axial shift mapping with no external measurement. The second extraction shown (Figure 6) is using an autocollimator to measure the tilts of the stage and then subtracting them out before comparing measurements. The final results are from using the known reference mirror in the field of view of the interferometer to measure tilts and removing the tilts before surface extraction (Figure 7). As mentioned above, shifting more than once better informs the Moore-Penrose inverse, so the raw data taken involved 40 shifts at 2 pixels per shift. This data is the average of 10 sets of these 40 shifts. The ultimate version of this method will involve less shifting and averaging, but we averaged this much to reduce random environmental error.

Both the reference surface and the SUT were extracted using a three-flat test once mounted in the aluminum mount. The ASM extracted surfaces are compared against the three-flat test extracted surface. We will not be able to characterize the SUT using the three-flat test once we transition to measuring curved optics with axial shift mapping, but currently this provides a great opportunity to compare results with a well-known and accepted metrology technique.

4.1 No external measurement

When no external measurement is used, we found there to be an rms difference of 33.1 nm for the reference surface and 29.9 nm for the SUT when comparing the surfaces to what was extracted using a three-flat test (Figure 5). Extracting the surfaces like this means that the quadratic shown in the surface can either be from a true quadratic term in the surface under test or can be from tilts during shifting. We cannot determine the origin because those two possibilities are degenerate in slope space. Extracting the surface without an external measurement illustrates the need for one if this method is to become reliable.

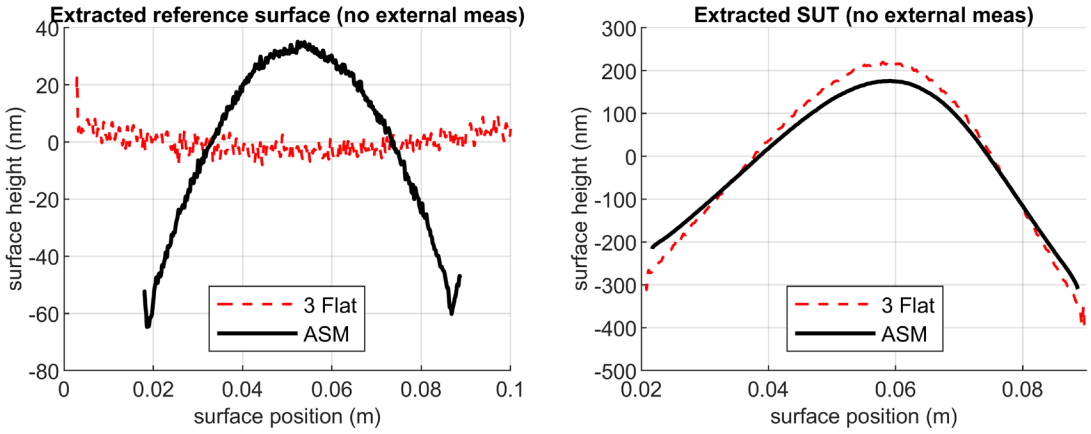

Figure 5. The extracted reference surface (*left*) and the extracted surface under test (*right*) when there is no external measurement to inform the quadratic term. The extracted surface in black is shown in comparison to the surface as measured by a three-flat test. The rms difference between the ASM extracted surface and the three-flat test extracted surface is 33.1 nm for the reference surface and 29.9 nm for the SUT.

4.2 Autocollimator external measurement

When using an autocollimator to remove the relative tilts between each measurement, the ASM extracted surface has an rms error of 14.2 nm for the reference surface and 13.3 nm for the SUT (Figure 6). We have shown better results in the past[18], but have since found the new numbers to reflect a more typical extraction that uses an autocollimator. One possible reason for the autocollimator to give good results during one measurement and less than ideal results the next is temperature fluctuations within the lab. The current experimental set up is not thermally isolated from ambient air and we have seen better result when taking data on Sundays. This corresponds to the lab coming to equilibrium after the building HVAC has been set at a fixed temperature for over 24 hours. We plan to explore other reasons why the autocollimator is not producing as repeatable results as we had expected as well.

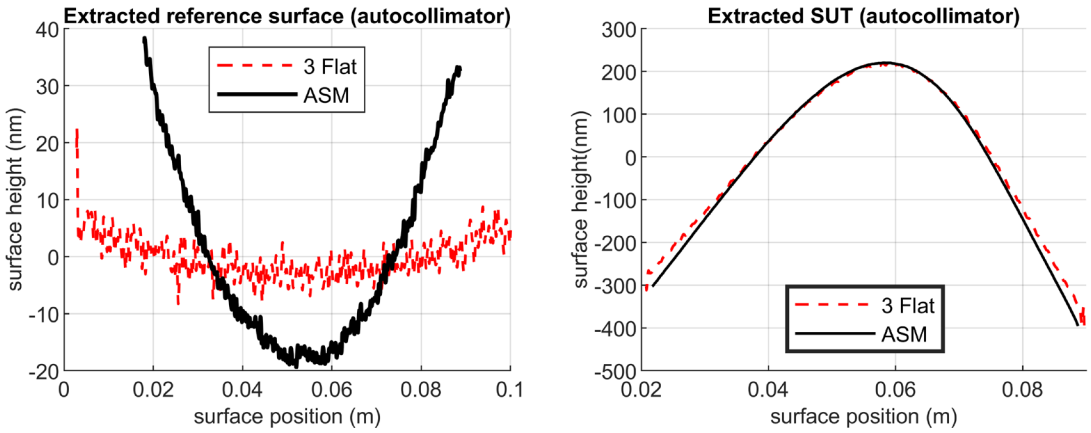

Figure 6. The extracted reference surface (*left*) and the extracted surface under test (*right*) when an autocollimator is used to eliminate the effects of tilts during shifting, informing the quadratic extraction. The rms difference between the ASM extracted surface and the three-flat test extracted surface is 14.2 nm for the reference surface and 13.3 nm for the SUT.

4.3 Reference mirror external measurement

We measured the best results when using the known reference mirror to extract relative tilts. We found the reference surface to have 4.6 nm rms error and the SUT to have 4.3 nm rms error (Figure 7). These measurements were repeated and we found the next measurement to also give sub-5 nm rms error. This meets the original goal of extracting the surface with rms error below 5 nm. As can be seen in Figure 7, there is still a deviation from the quadratic term as measured by the three-flat test. Despite that, we have found that using a reference mirror to be a more reliable and repeatable way to extract the SUT when compared to using an autocollimator. We believe that a lot of our current noise is due to having a ULE mirror in an aluminum mount. This large CTE mismatch could result in high temperature sensitivity, which is expected to be important over the 10 hour-long measurements presented here. This will be remedied in the future.

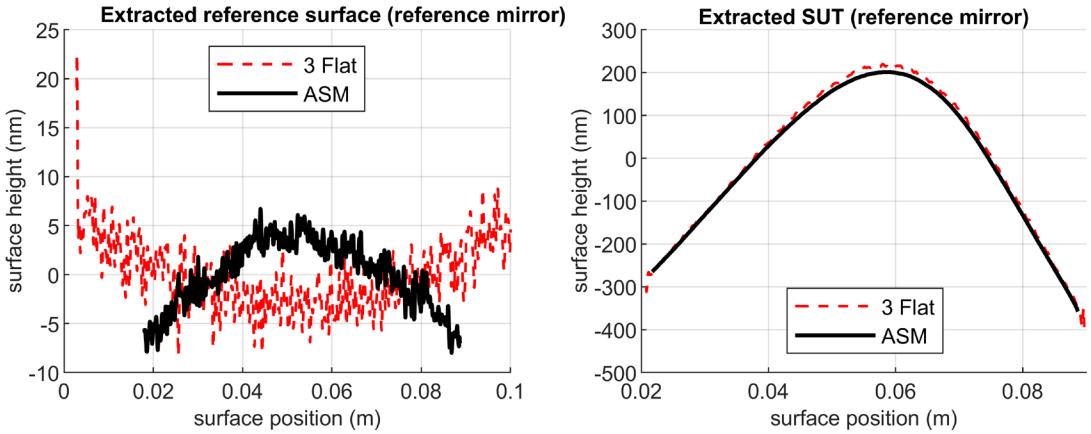

Figure 7. The extracted reference surface (*left*) and the extracted surface under test (*right*) when a premeasured reference mirror is used to eliminate tilts during shifting, informing the quadratic extraction. The rms difference between the ASM extracted surface and the three-flat test extracted surface is 4.6 nm for the reference surface and 4.3 nm for the SUT.

5. FUTURE WORK

We have begun designing our experiment that will move axial shift mapping from measuring flats to measuring curved, specifically acylindrical, surfaces. We plan to continue the use of the known reference mirror method to deal with the quadratic ambiguity that arises with axial shift mapping. In order to implement that tilt extraction method along with curved surfaces, we are considering an approach that relies on a computer-generated hologram (CGH). This CGH will generate the specific wavefronts that we need. Figure 8 shows the current CHG design that we are considering. This will

include a cylindrical or acylindrical wavefront from the center, and side wavefronts dedicated to our reference mirrors. The reference mirrors and the side wavefronts will be characterized using a three-flat test.

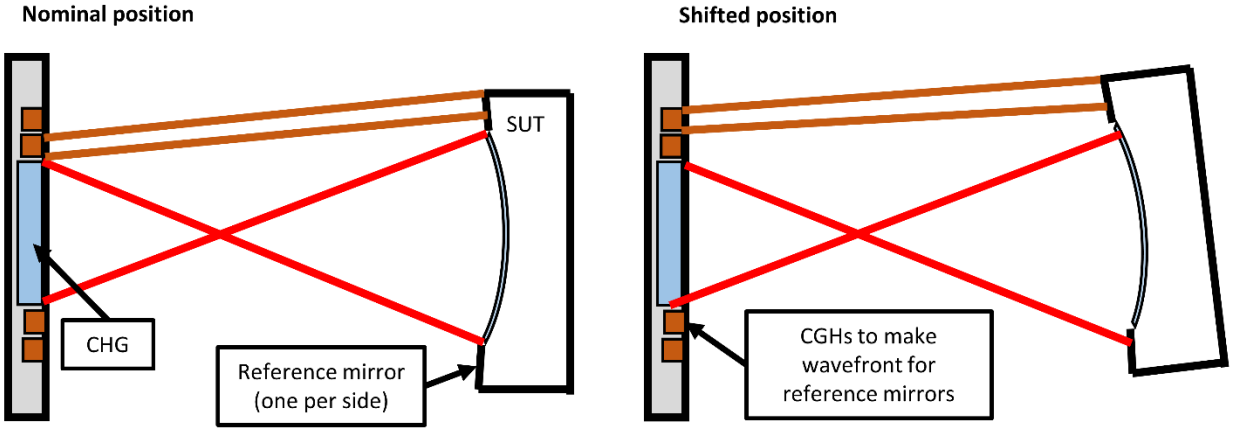

Figure 8. Diagram of current CGH design being considered. A central CGH will generate a cylindrical or acylindrical wavefront directed toward the SUT. On either side of the SUT there will be a reference mirror, each of which is accompanied by its own side CGH patterns. This will allow us to continue our method of using known reference mirrors while extending this method to X-ray mirrors.

We are building a ray trace program that will help determine the specific wavefront that we want the central CGH to generate. We can have the CGH designed to generate a wavefront that will match a cylinder, or to match a Wolter primary or secondary mirror of a specific radius. This decision will be based on the OPD that we see with each type of wavefront. Figure 9 shows preliminary results from our ray tracing, which demonstrates that with a cylindrical wavefront, neither a Wolter primary nor secondary mirror will generate too high of a fringe density for our Äpre Instruments S100 interferometer. We will continue to make our ray trace program more robust before making a final decision on the central wavefront.

The addition of the CGH to the system will allow us to continue to expand axial shift mapping from optical flats to acylindrical surfaces.

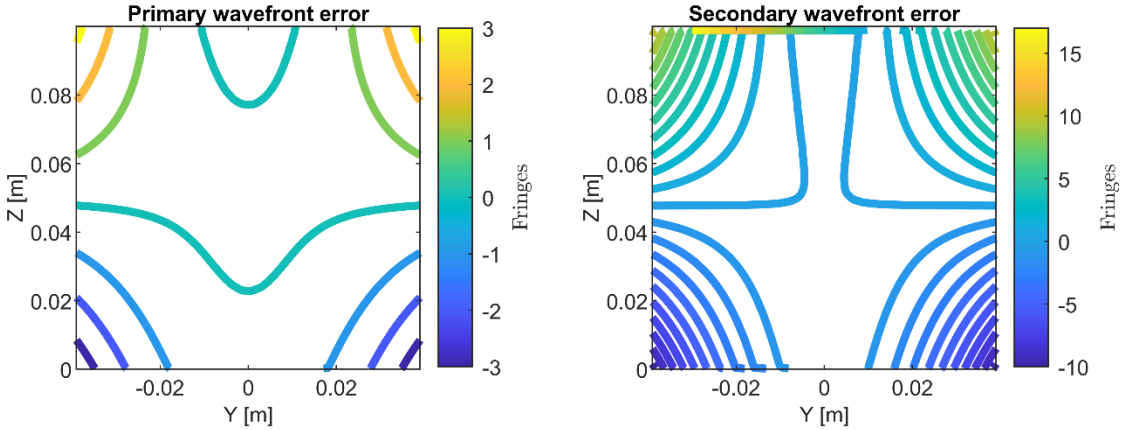

Figure 9. Preliminary results from our ray trace program showing the expected fringe pattern of a cylindrical wavefront from the CGH reflecting off of a Wolter primary and a Wolter secondary mirror (10 m focal length and 156 mm radius at mirror intersection). Both fringe patterns are low enough density that the Äpre Instruments S100 Fizeau interferometer will be able to measure the surface reliably.

6. CONCLUSION

We have shown results that we are able to extract a one-dimensional line of an optical flat to a sub-5 nm rms uncertainty using our new method of a known reference mirror in the field of view of the interferometer. We were able to extract the

reference surface with 4.6 nm rms error and the SUT with 4.3 nm rms error. We also showed that this method is more reliable than our previous method of using an autocollimator. A possible reason for the decreased performance when using the autocollimator was long term temperature drifting of the autocollimator. We will continue to develop the system for optical flats to explore the noise floor of this method. We also showed current developments of the system as we are beginning to move from optical flats to cylindrical and acylindrical surfaces.

This method will aid in creating well characterized acylindrical nulls which can be used in the manufacturing of the next generation of X-ray telescope mirrors, with the overall impact of aiding in the creation of a diffraction limited X-ray telescope.

ACKNOWLEDGEMENTS

We would like to thank Will Zhang at NASA Goddard Space Flight Center for engaging conversations while developing this method. This work was funded by NASA grant 80NSSC20K0907.

REFERENCES

[1] G. Vacanti, N. M. Barrière, M. J. Collon, E. Hauser, L. Babić, A. Bayerle, D. Girou, R. Günther, L. Keek, B. Landgraf, B. Okma, S. Verhoeckx, M. Vervest, L. Voruz, M. Bavdaz, E. Wille, M. Krumrey, P. Müller, and E. Handick, "X-ray testing of silicon pore optics," in Proc. SPIE 11119, p. 111190I. (2019).

[2] T. T. Saha, K.-W. Chan, J. R. Mazzarella, R. S. McClelland, P. M. Solly, W. W. Zhang, V. Burwitz, G. Hartner, M.-M. L. Caria, and C. Pelliciari, "Analysis of the NGXO telescope x-ray Hartmann data," in Proc. SPIE 10699, p. 1069952 (2018).

[3] J. P. Lehan, T. Hadjimichael, and C. Skocik, "Testing of the mirrors for the Constellation-X spectroscopy x-ray telescope with a refractive null," in Proc. SPIE, Vol. 6688, pp. 668819 (2007).

[4] J. P. Lehan, M. Atanossova, K.-W. Chan, T. Hadjimichael, T. T. Saha, M. Hong, W. W. Zhang, and P. Blake, "Progress toward a complete metrology set for the International X-ray Observatory (IXO) soft x-ray mirrors," in Proc. SPIE, Vol. 7437, pp. 74370R (2009).

[5] Y. Soong, T. Okajima, P. J. Serlemitsos, S. L. Odell, B. D. Ramsey, M. V. Gubarev, M. Ishida, Y. Maeda, R. Iizuka, T. Hayashi, Y. Tawara, A. Furuzawa, H. Mori, T. Miyazawa, H. Kunieda, H. Awaki, S. Sugita, K. Tamura, K. Ishibashi, T. Izumiya, S. Minami, T. Sato, K. Tomikawa, N. Kikuchi, and T. Iwase, "ASTRO-H Soft X-ray Telescope (SXT)," in Proc. SPIE, Vol. 9144, p. 914428 (2014).

[6] H. Li, P. Z. Takacs, and T. Oversluizen, "Vertical scanning long trace profiler: a tool for metrology of x-ray mirrors," in Proc. SPIE, Vol. 3152, pp. 180–188 (1997).

[7] M. V. Gubarev, T. Kester, and P. Z. Takacs, "Calibration of a vertical-scan long trace profiler at MSFC," in Proc. SPIE, Vol. 4451, pp. 333–340 (2001).

[8] R. Allured et al., "Measuring the performance of adjustable x-ray optics with wavefront sensing," Proc. SPIE 9144, 91441D (2014).

[9] C. R. Forest, C. R. Canizares, D. R. Neal, M. McGuirk, and M. L. Schattenburg, "Metrology of thin transparent optics using Shack-Hartmann wavefront sensing," Opt. Eng 43(3), 742–753 (2004).

[10] K. Kilaru, B. D. Ramsey, W. H. Baumgartner, S. D. Bongiorno, D. M. Broadway, P. R. Champey, J. M. Davis, S. L. O'Dell, R. F. Elsner, J. A. Gaskin, S. Johnson, J. K. Kolodziejczak, O. J. Roberts, D. A. Swartz, and M. C. Weisskopf, "Full-shell x-ray optics development at NASA Marshall Space Flight Center," J. Astron. Telesc. Instrum. Syst. 5(2), (2019).

[11], J. A. Gaskin et al., "Lynx X-Ray Observatory: an overview," J. of Astronomical Telescopes, Instruments, and Systems. 5(2), (2019).

[12] W. W. Zhang, K. D. Allgood, M. Biskach, K.-W. Chan, M. Hlinka, J. D. Kearney, J. R. Mazzarella, R. S. McClelland, A. Numata, R. E. Riveros, T. T. Saha, and P. M. Solly, "High-resolution, lightweight, and low-cost x-ray optics for the Lynx observatory," J. Astron. Telesc. Instrum. Syst. 5(2), 021012 (2019).

[13] L. P. VanSpeybroeck, and R. C. Chase, "Design Parameters of Paraboloid-Hyperboloid Telescopes for X-ray Astronomy," Appl. Opt. 11, 440-445 (1972).

[14] G. Schulz and J. Schwider, “IV Interferometric Testing of Smooth Surfaces,” Progress in Optics 13, 118-140 (1976).

[15] D. Su, E. Miao, Y. Sui, and H. Yang, "Absolute surface figure testing by shift-rotation method using Zernike polynomials," Opt. Lett. 37, 3198-3200 (2012).

[16] E. E. Bloemhof, “Absolute surface metrology by differencing spatially shifted maps from a phase-shifting interferometer,” Opt. Lett. 35(14), 2346-2348 (2010).

[17] E. E. Bloemhof, “Absolute surface metrology with a phase-shifting interferometer for incommensurate transverse spatial shifts,” Opt. Lett. 53(5), 792-797 (2014).

[18] H. J. Wisniewski, M. M. Whalen, R. K. Heilmann, M. L. Schattenburg, B. D. Chalifoux “Lateral shift mapping for X-ray telescope mirrors”, Proc. SPIE 11822, 118220X (2021).